Effects of the anomalous Higgs couplings on the Higgs boson production at the Large Hadron Collider

Kanemura, Shinya
Department of Physics, University of Toyama

TSUMURA, KOJI
The Abdus Salam ICTP of UNESCO and IAEA

Effects of the anomalous Higgs couplings on the Higgs boson production at the Large Hadron Collider

Shinya Kanemura[1,∗] and Koji Tsumura[2,†]

¹Department of Physics, University of Toyama,

3190 Gofuku, Toyama 930-8555, Japan

²The Abdus Salam ICTP of UNESCO and IAEA,

Strada Costiera 11, 34151 Trieste, Italy

Abstract

We study the impact of dimension-six operators on single- and double-Higgs production rates via gluon fusion at the Large Hadron Collider (LHC). If the top-Yukawa coupling is modified by some new physics whose scale is of the TeV scale, its effect changes the cross sections of single-Higgs production $gg \to H$ and double-Higgs production $gg \to HH$ through the top-loop diagram. In particular, double-Higgs production can receive significant enhancement from the effective top-Yukawa coupling and the new dimension-five coupling $t\bar{t}HH$ which are induced by the dimension-six operator. Comparing these results to the forthcoming data at the LHC, one can extract information of the dimension-six operators relevant to the top quark and the Higgs boson.

∗Electronic address: kanemu@sci.u-toyama.ac.jp

†Electronic address: ktsumura@ictp.it

arXiv:0810.0433v2 [hep-ph] 2 Aug 2009

I. INTRODUCTION

Gauge symmetries of the standard model (SM) have been well confirmed at the CERN Large Electron Positron collider (LEP) [1] and the Fermilab TEVATRON. However the mechanism of spontaneous symmetry breaking has not been tested yet [2, 3]. The vacuum expectation value of the Higgs boson triggers electroweak symmetry breaking and generates masses of weak gauge bosons, quarks and charged leptons. Search for the Higgs boson is the main purpose of the measurement at the CERN Large Hadron Collider (LHC).

In the SM, coupling constants of the Higgs boson with the weak gauge bosons and the matter fields directly relate to their masses. In order to clarify the mass generation mechanism, an independent determination of the particle masses and their couplings to the Higgs boson is important, which will be the subsequent task at the LHC. It will give not only a confirmation of the SM but also an indication of new physics beyond the SM.

At the LHC the dominant production mechanism of the Higgs bosons is gluon fusion $gg \to H$. The leading contribution to this process comes from top-quark loop diagrams. Information of the top-Yukawa coupling can be extracted through this process as a combination with the Higgs decay branching ratios. The gauge interaction of the Higgs boson would be tested through processes of vector boson fusion $VV^* \to H(V = W^-, Z)$ [4, 5] and Higgs-strahlung $q\bar{q}' \to VH$ [6]. These processes are promising channels for Higgs searches too because of the kinematic advantage in the reconstruction of signals. Measurement of the triple-Higgs boson coupling has been discussed in the double-Higgs production mechanism from gluon fusion, $gg \to HH$, at the LHC [7]. In Ref. [8] the sensitivity to the Higgs boson self-coupling is studied. The authors of this reference conclude that its experimental accuracy could reach 20–30% at the SLHC with an integrated luminosity of $L = 3000$ fb^{-1} for $m_H = 150$–200 GeV.

Measuring the top-Yukawa coupling accurately is important because the magnitude of the coupling constant $(y_t^{\mathrm{SM}} \sim 1)$ indicates that the physics of top quarks closely would relate to that of electroweak symmetry breaking. Lots of models are proposed in this direction [9]. Measurements of the top-Yukawa coupling would be a key to uncover such possibilities. In addition, the Higgs boson self-coupling is of great interest by itself to understand the nature of spontaneous symmetry breaking. Its measurement can also be a probe of the new physics beyond the SM. The coupling strength is also important being deeply related to the

condition of successful electroweak baryogenesis[10].

New physics beyond the SM will be recognized by the discovery of non-SM particles or by detecting the deviation from the SM relations between masses and coupling constants. For the latter case, the low energy effective theory at the electroweak scale can be described by the SM Lagrangian with additional higher dimensional operators. This approach has been investigated to analyze non-standard interactions in a model independent way. Leading order contributions of such non-standard interactions would be described by the dimension-six operators [11]. Constraints on these operators and their phenomenology have been discussed in the literature [12, 13, 14].

In this paper, we study new physics effects from dimension-six operators on single- and double-Higgs production processes, $gg \to H$ and $gg \to HH$. The dimension-six operators correct to the top-Yukawa coupling and the triple-Higgs boson coupling, also induce the tree level ggH and $ggHH$ vertices. Effects due to the modified top-Yukawa coupling and the tree level coupling on the effective ggH vertex are investigated. The former comes from color blind new dynamics while the latter can come from some color dependent effects. The experimental limits from the LEP precision data and the theoretical bounds such as the unitarity bounds are taken into account. We find that the effects on these processes due to the dimension-six operators can be significant even under these constraints. In particular the double-Higgs production cross section is sensitive to these dimension-six operators. These contributions from the dimension-six operators can be distinguished by comparing the data for these Higgs boson production channels at the LHC experiments.

This paper is organized as follows. In Sec. II, we introduce the dimension-six operators as a new physics effect. Its experimental and theoretical bounds are discussed. In Sec. III, numerical evaluations of the effects of dimension-six operators on the Higgs production processes at the LHC are shown. Conclusions and discussions are given in Sec. IV. A detailed calculation is shown in the appendix.

II. EFFECTIVE LAGRANGIAN

New physics effects on phenomena at the electroweak scale can be described by the higher dimensional operators [11]. The effective Lagrangian is given by

$$\mathcal{L}_{\text{eff}} = \mathcal{L}_{\text{SM}} + \sum_i \sum_{n \geq 5} \frac{C_i}{\Lambda^{n-4}} \mathcal{O}_i^{(n)}, \tag{1}$$

where $\mathcal{L}_{\text{SM}}$ is Lagrangian of the SM, C_i are the coupling strengths of the dimension-n operators $\mathcal{O}_i^{(n)}$, and Λ is a cut off scale of the SM. The coefficients of these higher dimensional operators can in principle be calculated by assuming new physics models which are defined above the scale Λ. When Λ is much greater than the electroweak scale, the dimension-six operators can give leading contributions to the deviations from the SM.

If the top-Yukawa interaction is modified by the dimension-six operators, its effect can be observed in the processes of $gg \to H$ and $gg \to HH$. The dimension-six operators relevant to the gluon fusion mechanism are

$$\mathcal{O}_{t1} = \left(\Phi^\dagger \Phi - \frac{v^2}{2} \right) \left(\overline{Q}\, t_R\, \widetilde{\Phi} + \widetilde{\Phi}\, \overline{t_R}\, Q \right), \tag{2}$$

$$\mathcal{O}_{Dt} = \left(\overline{Q}\, D_\mu\, t_R \right) D^\mu \widetilde{\Phi} + \left(D^\mu \widetilde{\Phi} \right)^\dagger \left(\overline{D_\mu\, t_R}\, Q \right), \tag{3}$$

$$\mathcal{O}_{tG\Phi} = \left[\left(\overline{Q}\, \sigma^{\mu\nu} \lambda^A\, t_R \right) \widetilde{\Phi} + \widetilde{\Phi}^\dagger \left(\overline{t_R}\, \sigma^{\mu\nu} \lambda^A\, Q \right) \right] G_{\mu\nu}^A, \tag{4}$$

where $Q = (u, d)_L^T$, $G_{\mu\nu}^A$ is the field strength of gluons with $SU(3)$ generators $\lambda^A (A = 1\text{–}8)$, Φ is a scalar-iso-doublet with hypercharge $Y = 1/2$, $\widetilde{\Phi} = i\, \tau_2 \Phi^*$, and v (~ 246 GeV) is the vacuum expectation value whose origin may come from color blind dynamics. The effective top-Yukawa coupling deviates from the SM value due to $\mathcal{O}_{t1}$ and $\mathcal{O}_{Dt}$. There is only one dimension-six operator $\mathcal{O}_G$ [15] that contributes to ggH and $ggHH$ vertices at the tree level; i.e.,

$$\mathcal{O}_G = \left(\Phi^\dagger \Phi - \frac{v^2}{2} \right) G_{\mu\nu}^A G^{A\mu\nu}, \tag{5}$$

whose origin can come from colored new dynamics at the TeV scale.

The triple-Higgs boson coupling also contributes to double-Higgs production $gg \to HH$. Dimension-six genuine-Higgs operators change the Higgs self-coupling, which are given

by [14]

$$\mathcal{O}_{\Phi 1} = \frac{1}{2} \partial_\mu \left(\Phi^\dagger \Phi \right) \partial^\mu \left(\Phi^\dagger \Phi \right), \tag{6}$$

$$\mathcal{O}_{\Phi 2} = -\frac{1}{3} \left(\Phi^\dagger \Phi \right)^3, \tag{7}$$

$$\mathcal{O}_{\Phi 3} = \left(D_\mu \Phi \right)^\dagger \Phi \, \Phi^\dagger \left(D^\mu \Phi \right). \tag{8}$$

Normalization of the Higgs field is shifted by introduction of the operator $\mathcal{O}_{\Phi 1}$. All the Higgs interactions are corrected after the wave function renormalization for the Higgs boson [14]. The Higgs potential is modified by $\mathcal{O}_{\Phi 2}$; then the triple-Higgs boson coupling is a function of $C_{\Phi 2}$ and the Higgs boson mass. The coefficient $C_{\Phi 2}$ simply shifts the triple-Higgs coupling.

The coefficients C_{t1}, $C_{\Phi 1}$ and $C_{\Phi 2}$ are free from the current experimental data[1]. In contrast, the coefficient of $\mathcal{O}_{\Phi 3}$ ($\mathcal{O}_{Dt}$) contributes to the electroweak rho parameter at the tree level (and the one-loop level), which is strongly constrained by the experimental data [13, 16]. The effects of $\mathcal{O}_{tG\Phi}$ will be measured by top-pair production, $gg \to t\bar{t}$. Here we neglect the operators $\mathcal{O}_{Dt}$, $\mathcal{O}_{tG\Phi}$ and $\mathcal{O}_{\Phi 3}$ in the following discussion assuming that these operators would be well constrained by the other processes, and we concentrate on the effects due to the operators $\mathcal{O}_{t1}, \mathcal{O}_{\Phi 1}, \mathcal{O}_{\Phi 2}$ and $\mathcal{O}_G$. In Ref. [15], the bounds on the operator $\mathcal{O}_G$ are evaluated through the process $gg \to H \to WW$ for $m_H \gtrsim 160$ GeV,

$$-1.2 \lesssim a_G \left(\frac{\alpha_s}{4\pi} \right)^{-1} \lesssim 0.5, \tag{9}$$

where the scaled couplings are defined as $a_i = C_i \frac{v^2}{\Lambda^2}$.

The theoretical upper bounds on these operators from tree level unitarity [17] have been discussed in the literature [14, 18]. Such bounds on these less constrained operators are given by

$$a_{t1} \lesssim \frac{16\pi}{3\sqrt{2}} \frac{v}{\Lambda}, \tag{10}$$

$$a_{\Phi 1, \Phi 2} \lesssim 4\pi \frac{v^2}{\Lambda^2}. \tag{11}$$

If we consider the low energy cut off $\Lambda = 1$–3 TeV, the upper bound on a_{t1} are 3.0–1.0, respectively [14].

---

[1] The coefficient $C_{\Phi 1}$ would be determined precisely at the ILC by using the gauge boson association processes such as Higgs-strahlung and vector boson fusion.
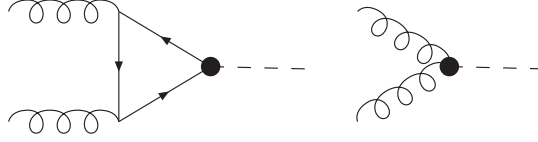
FIG. 1: Feynman diagrams for the single-Higgs production process via gluon fusion. Curled, dashed and solid lines represent gluons, Higgs bosons and quarks, respectively. Dots denote the new physics interaction. In the SM, there is no tree level contact interaction.

Set	A	B	C	D	E	F
a_{t1}	0	+0.5	−0.5	0	0	0
a_G	0	0	0	+0.004	−0.004	0
$a_{\Phi 2}$	0	0	0	0	0	+0.5

TABLE I: Parameter sets for the coefficients of the dimension-six operators.

III. NUMERICAL EVALUATION OF THE HIGGS PRODUCTION PROCESSES

By introducing the dimension-six operators $\mathcal{O}_{t1}$ and $\mathcal{O}_{\Phi 1}$, the effective top-Yukawa coupling is expressed as

$$y_t^{\text{eff}} = Z_{\Phi 1} \left(\frac{\sqrt{2} m_t}{v} - a_{t1} \right), \tag{12}$$

where $Z_{\Phi 1} = (1 + a_{\Phi 1})^{-1/2}$. Feynman diagrams for single-Higgs production via gluon fusion is depicted in FIG. 1. For $a_G = 0$, the new physics contribution to this process only appears in the effective top-Yukawa coupling. Therefore $gg \to H$ only depends on a_{t1} and $a_{\Phi 1}$ by the combination given in Eq. (12). We here define the parameter sets; Set A–Set F, for the coefficients of dimension-six operators in TABLE I. Set A corresponds to the SM. The effects of $\mathcal{O}_{t1}$ are studied by Set B and Set C, and those of $\mathcal{O}_{t1}$ are investigated by Set D and Set E. Set F shows those of $\mathcal{O}_{\Phi 2}$. The values of $a_{t1} = \pm 0.5$ correspond to the unitarity bounds for $\Lambda = 5$ TeV, which change the effective top-Yukawa coupling by about 50%. If we take a lower cut off scale ($\Lambda < 5$ TeV), the unitarity constraint on a_{t1} becomes milder.

The hadronic production cross section for $pp \to ggX \to HX$ is evaluated as a function of m_H at the LHC in FIG. 2. Detailed calculations are shown in Appendix A. The solid, dotted, dashed, long-dashed and dot-dashed curves correspond to the parameter sets Set A–Set E, respectively. The peak around $m_H \sim 350$ GeV in these curves is understood as
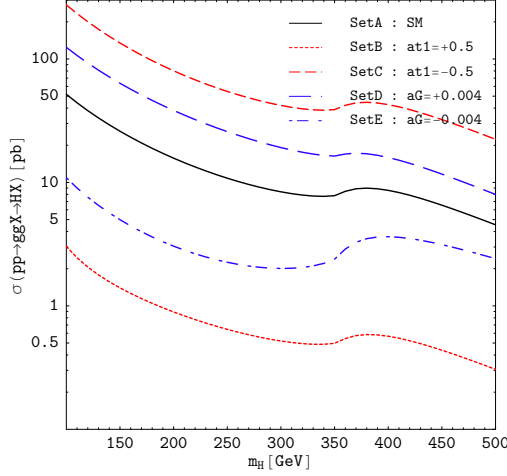
FIG. 2: The cross section of $pp \to ggX \to HX$ with $\sqrt{s} = 14$ TeV as a function of the Higgs boson mass. Curves denote the cross sections derived in the SM (Set A), and in the SM with anomalous dimension-six couplings (Set B–Set E).

the threshold effect due to the top-quark loop. If the effective top-Yukawa coupling deviates from its SM value (Set B and Set C), the cross section can be enhanced by a factor $\sim 9/4$ or suppressed by $\sim 1/4$ for entire range of the Higgs boson mass. These effects are determined only by y_t^{eff}. The differences from the SM for Set D and Set E are comparable to that for top-Higgs coupling for Set B and Set C around $m_H \sim 120$ GeV. The effects on the cross section from Set D and Set E are relatively small compared to Set B and Set C for the larger Higgs boson masses. These structures are realized by the interference of the amplitudes between the new physics contributions and the SM one.

In FIGs. 3 and 4, we evaluate the statistical sensitivities for anomalous parameters on $N = L\,\sigma(pp \to ggX \to HX)\mathcal{B}(H \to WW, \gamma\gamma)$ where the integrated luminosity is assumed to be $L = 300\text{fb}^{-1}$. The efficiencies of W bosons and photons are taken as 100% for the illustration. Therefore, in these plots, the $H \to WW$ decay mode always gives a better sensitivity than the $H \to \gamma\gamma$ decay mode because the decay branching ratios hold the relation $\mathcal{B}(H \to WW) \gg \mathcal{B}(H \to \gamma\gamma)$ for $m_H \gtrsim 100$ GeV. Note that we do not include any backgrounds to calculate the statistical sensitivity. For larger Higgs boson masses, the sensitivities become worse due to the decreasing of the cross section. For the WW decay mode with $m_H \lesssim 120$ GeV, it has also bad sensitivities because of the small branching
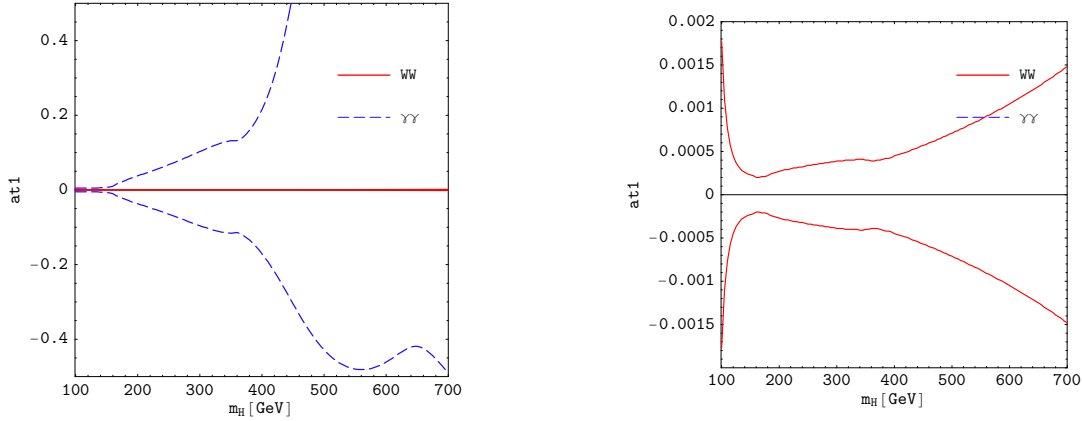
FIG. 3: The plot of the statistical sensitivity for a_{t1} on $N = L\sigma(pp \to ggX \to HX)\mathcal{B}(H \to WW, \gamma\gamma)$ where the integrated luminosity is $L = 300\text{fb}^{-1}$. Each curve denotes the 1σ deviation from the SM predictions.
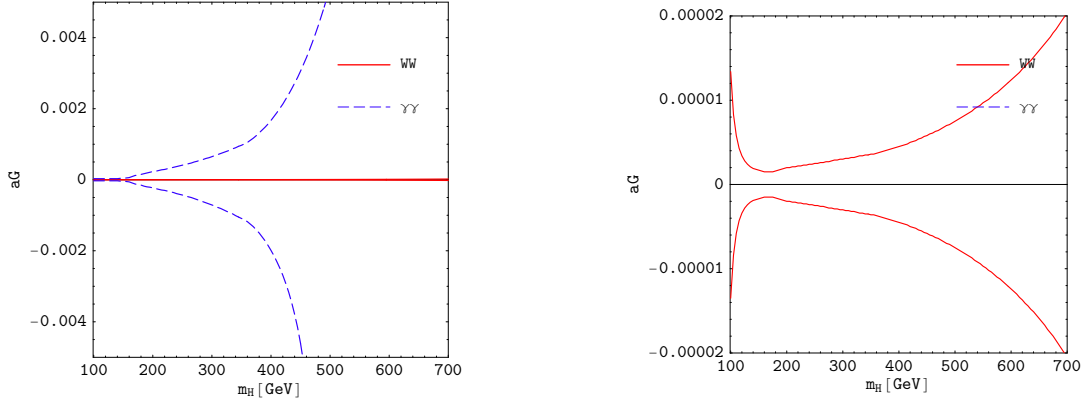

FIG. 4: The plot of the statistical sensitivity for a_G on $N = L\sigma(pp \to ggX \to HX)\mathcal{B}(H \to WW, \gamma\gamma)$ where the integrated luminosity is $L = 300\text{fb}^{-1}$. Each curve denotes the 1σ deviation from the SM predictions.

fraction of $H \to WW$.

In FIG. 5, we show the contour plot of the sensitivities in the a_{t1}–a_G plane. There is a strong correlation between a_{t1} and a_G. This means that a_{t1} can mimic the effect of a_G in this process. It is understood by the destructive interference of the top-loop diagram, which is shifted by a_{t1} and the *tree level* diagram, which is induced by the dimension-six operator
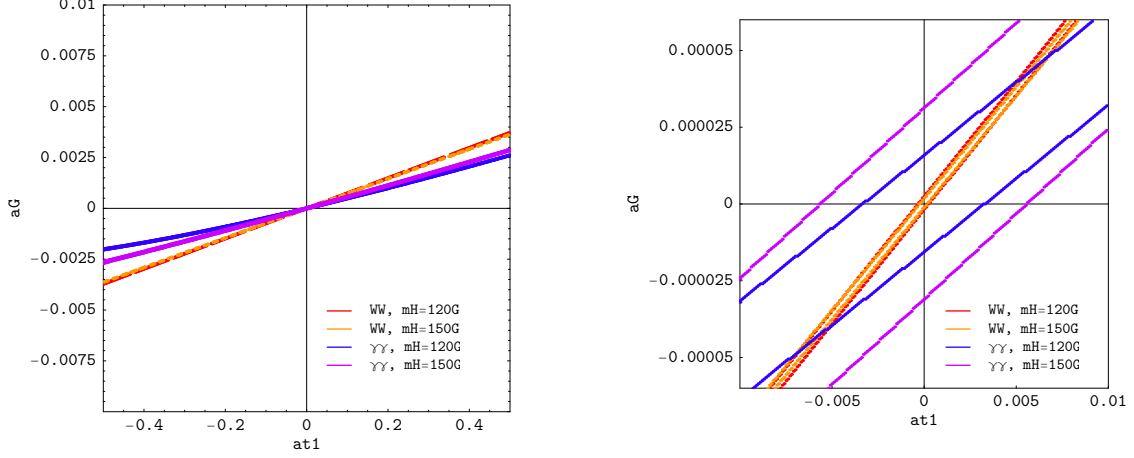
FIG. 5: The sensitivity plots in the a_{t1}–a_G plane on $N = L\,\sigma(pp \to ggX \to HX)\mathcal{B}(H \to WW, \gamma\gamma)$ where the integrated luminosity is $L = 300\text{fb}^{-1}$. Each contour represents the 1σ deviation from the SM predictions.
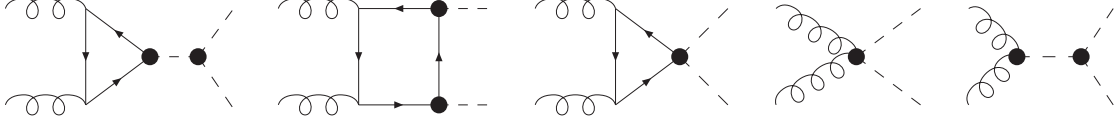

FIG. 6: Feynman diagrams for the double-Higgs production process $gg \to HH$ are depicted. Dots represent the new vertices of the dimension-six operators.

$\mathcal{O}_G$. Therefore, if the deviation from the SM is found in $gg \to H$, we cannot distinguish the effects of these anomalous couplings.

Next, let us discuss the double-Higgs production. In FIG. 6, we show the Feynman diagrams for the process $gg \to HH$. Invariant amplitudes for the sub-process are given in Appendix A. For each diagram, appropriate crossing of external Higgs-boson and gluon lines should be taken into account. In the SM, there are only two kinds of topology, the first and second diagrams from the left. This process would be used to measure the triple-Higgs boson coupling at the SLHC. The vertex function of HHH is modified by the introduction of the genuine Higgs operators as

$$\lambda_{HHH}(\hat{s}) = Z_{\Phi 1}^{3/2}\left(Z_{\Phi 1}^{-1}\frac{m_H^2}{2v^2} - \frac{\hat{s} + 2m_H^2}{v^2}a_{\Phi 1} + \frac{a_{\Phi 2}}{3}\right)v, \tag{13}$$

where $\sqrt{\hat{s}}$ is the center of mass energy of $gg \to HH$. For Set F, the coefficient $a_{\Phi 2}$ is taken to be positive to ensure vacuum stability. The value $a_{\Phi 2} = +0.5$ corresponds to the 140%
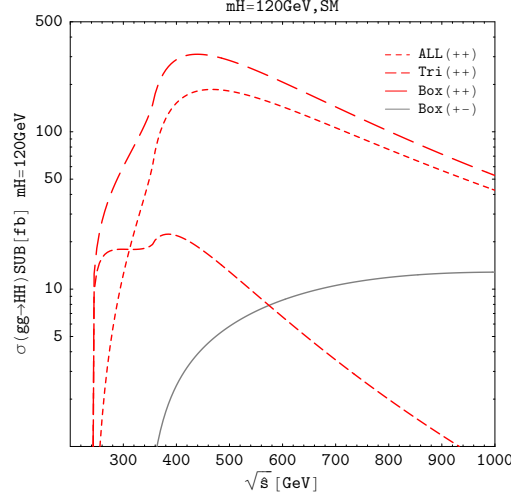
9

FIG. 7: The cross section for the Higgs pair production sub-process $gg \rightarrow HH$ as a function of scattering energy for $m_H = 120$ GeV in the SM. The dashed (long-dashed) curve denotes the contribution coming from the triangle (box) diagram with the $(+,+)$ helicity set of gluons. The dotted curve is a composition of these two. The thin solid one represents the helicity set $(+,-)$ in the box diagram.

enhancement of the triple-Higgs boson coupling for $m_H = 120$ GeV.

The cross sections for the Higgs boson pair production via the gluon fusion sub-process are shown in FIG. 7 in the SM. The dotted and thin solid curves represent the cross section with the helicity set $(+,+)$ and $(+,-)$ of the gluons. For $m_H = 120$ GeV, the main contribution comes from the box diagram (long-dashed) because the triangle diagram (dashed) contains the Higgs boson self-coupling, which is proportional to the Higgs boson mass squared, and it has the typical behavior of the s-channel process.

In FIG. 8, we show the effect of the dimension-six top–Higgs interaction on $gg \rightarrow HH$ as a function of m_H for Set B and Set C. These curves are used as the same manner as in FIG. 8. The additional long-dot-dashed curve represents new vertex contribution. The SM with gluon helicity sets $(+,+)$ and $(+,-)$ are also shown in thick and thin solid curves. For Set B, it can be seen that the effective top-Yukawa coupling is suppressed in both the triangle and the box diagrams. The cross section can also be enhanced by the dimension-five interaction vertex of $t\bar{t}HH$ due to $\mathcal{O}_{t1}$. On the contrary, for Set C the contributions from the box diagrams become large because of the large effective top-Yukawa coupling. The synergy
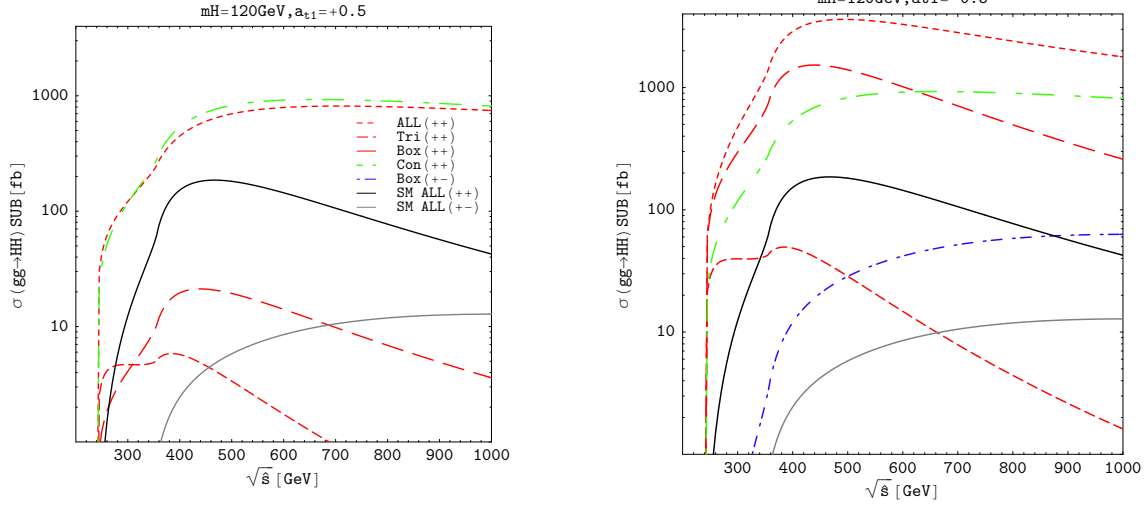
FIG. 8: The cross section for the process $gg \to HH$ as a function of $\sqrt{\hat{s}}$ for $m_H = 120$ GeV for Set B and C. Each curve is given in the same manner as in FIG. 7. The long-dot-dashed curve denotes the contribution comes from the new vertex which is induced by the dimension-six operator. The SM with helicity sets $(+, +)$ and $(+, -)$ of the gluons are also shown in thick and thin solid curves as a reference.
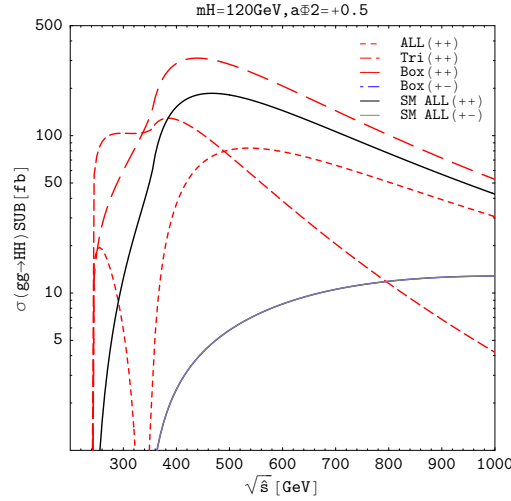

FIG. 9: The cross section of $gg \to HH$ for $m_H = 120$ GeV with $a_{\Phi2} = +0.5$ as a function of $\sqrt{\hat{s}}$. The curves are defined in the same manner as FIG. 8.

effect of both the contributions enhances the sub-process cross section significantly.

In FIG. 9, we show the $gg \to HH$ cross section as a function of $\sqrt{\hat{s}}$ for Set F. Each curve is given as in FIG. 8. The contribution of $a_{\Phi2}$ only appears in the triple-Higgs boson vertex.
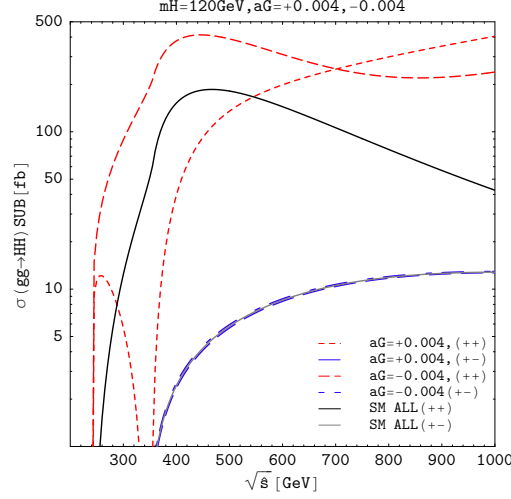
11

FIG. 10: The cross section of $gg \to HH$ as a function of sub-process energy for $m_H = 120$ GeV in the SM with $a_G = \pm 0.004$. The dotted and long-dashed curves denote the gluon helicity sets $(+, +)$ and $(+, -)$ for Set D. The dashed and dot-dashed curves are those for Set E. The SM predictions are also given by solid curves.

Around $m_H \sim 350$ GeV, a strong destructive interference between the triangle and the box diagrams occurs. The effect in Set F is relatively small as compared to those in Set B and Set C. There is also enhancement on the sub-process cross section near the threshold of HH production. These effects turn out to give larger contributions to the hadronic cross section.

For completeness, we also show the case for Set D and Set E in FIG. 10. The dotted and long-dashed curves represent the helicity set $(+, +)$ and $(+, -)$ of gluons for Set D. Those for Set E are given by the dashed and dot-dashed curves. The SM prediction is also shown. For Set D, there is a cancellation between the SM contribution and the anomalous tree level vertex ggH in the $t\bar{t}$ threshold region. In Set E, each contribution is constructive in the same parameter region.

Convoluting the CTEQ6M parton distribution function [19], the full cross section is evaluated for double-Higgs production via gluon fusion. In FIG. 11, we show the hadronic cross sections as a function of the Higgs boson mass in the left figure and as a function of the dimension-six couplings in the right figure. Significant enhancement from the dimension-six operators $\mathcal{O}_{t1}$ and $\mathcal{O}_G$ can be seen in both figures for a wide range of parameter space. For Set F, the curve and that of the SM one coincide for large m_H values whose structure is
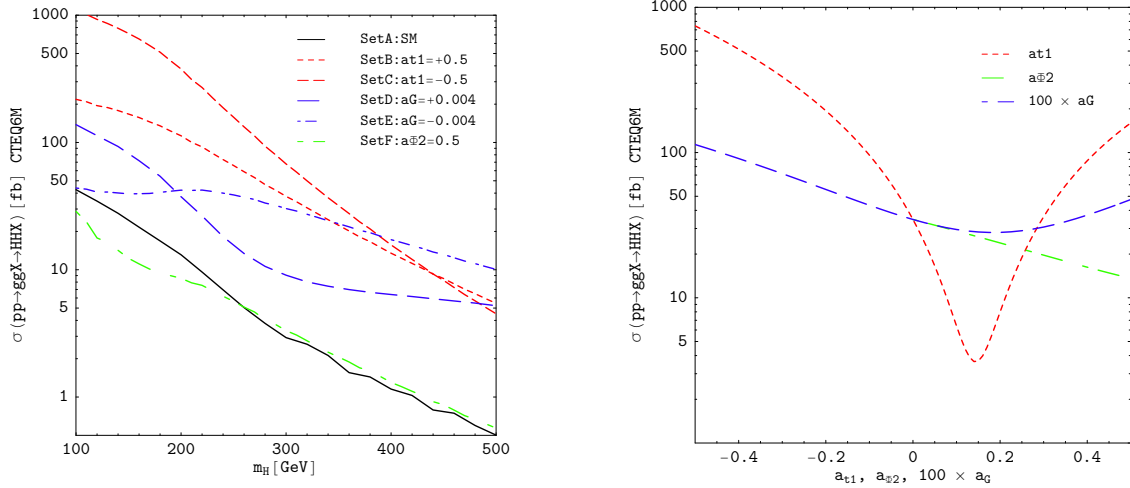
FIG. 11: The total cross section of the double-Higgs production $pp \to ggX \to HHX$ as a function of the Higgs boson mass in the left figure and the anomalous couplings in the right figure with center of mass energy $\sqrt{s} = 14$ TeV.

easily understood from Eq. (13). The effect of $a_{\Phi 2}$ is reduced when we take larger Higgs boson masses. The contributions from $a_{\Phi 1}$ might be much larger than those of the other operators. This effect will be first examined by gauge boson association processes.

In FIG. 12, we evaluate the statistical sensitivities for the anomalous parameters on $N = L\,\sigma(pp \to ggX \to HHX)\mathcal{B}(H \to WW)\mathcal{B}(H \to WW)$ where the integrated luminosity is assumed to be $L = 300\text{fb}^{-1}$. We focus on the anomalous parameters a_{t1} and a_G, because this process is insensitive to $a_{\Phi 2}$ as we showed in FIG. 11. Obtained sensitivities are less smaller than those in $gg \to H$ process. However, this process is still sensitive to a_{t1} for $m_H \sim 150$ GeV on some level due to the large enhancement (suppression) in the box diagram. On the other hand, it is insensitive to the anomalous parameter a_G.

We show the contour plot of the sensitivities in the a_{t1}–a_G plane in FIG. 13. To compare the single- and double-Higgs production processes, we also show the results calculated from $gg \to H$. By using the insensitivity of $gg \to HH$ to a_G, the anomalous parameter a_{t1} can be constrained.

The possibility of measuring the Higgs boson pair production has been discussed in Ref. [8] to determine the triple Higgs boson coupling constant. Their background analyses can apply to our setup because the dominant decay modes of the Higgs boson are almost the same as in the SM. In our case, the double-Higgs production process can be observable if the cross
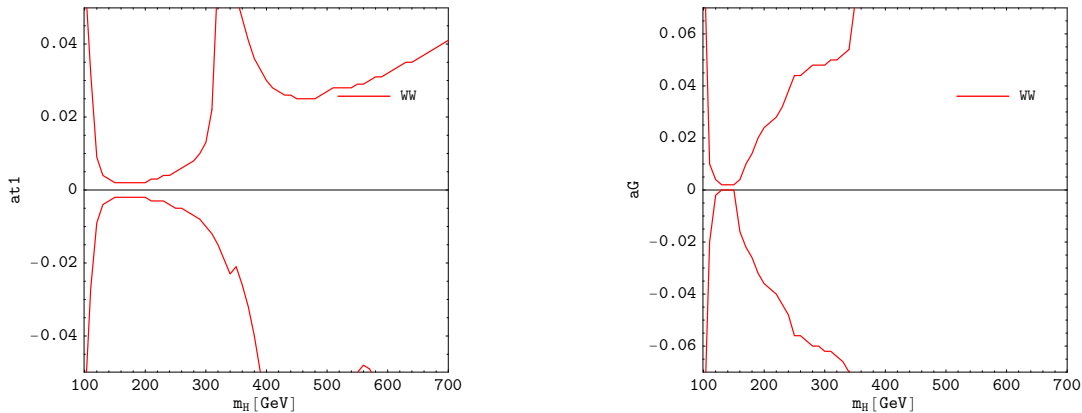
13

FIG. 12: The plot of the statistical sensitivity for a_{t1} on $N = L\sigma(pp \to ggX \to HHX)\mathcal{B}(H \to WW)\mathcal{B}(H \to WW)$ where the integrated luminosity is $L = 300\text{fb}^{-1}$. Each curve denotes the 1σ deviation from the SM predictions.

section receives the above enhancement. However it does not mean the improvement of the sensitivity for the triple-Higgs boson coupling. The new vertex $t\bar{t}HH$ smears the effect of the Higgs boson self-coupling. We find that $gg \to HH$ can still be sensitive to the dimension-six top-Higgs interaction.

IV. CONCLUSIONS AND DISCUSSIONS

In this paper, we have studied the impact of the dimension-six operators on the Higgs production processes via gluon fusion, i.e., $gg \to H$ and $gg \to HH$ at the LHC. Constraints from the current experimental data and the theoretical consistencies on the dimension-six operators are taken into account. We find that the contribution from the dimension-six top–Higgs operators to single-Higgs production can significantly change the cross section by a factor. The double-Higgs production process can also receive a large enhancement from the anomalous top-Higgs couplings. The shift of the effective top-Yukawa coupling can enhance the cross section significantly. In addition, the new diagrams from the tree level vertex $t\bar{t}HH$ from $\mathcal{O}_{t1}$ result in much larger cross sections than that in the SM. Combined results of single- and double-Higgs production can be used to discriminate between the effects of dimension-six operators $\mathcal{O}_{t1}$ and $\mathcal{O}_G$.
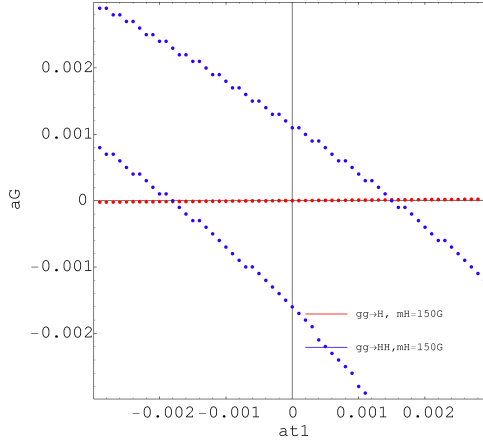
14

FIG. 13: The sensitivity plots in the a_{t1}–a_G plane on $N = L\,\sigma(pp \to ggX \to HHX)\mathcal{B}(H \to WW)\mathcal{B}(H \to WW)$ where the integrated luminosity is $L = 300\text{fb}^{-1}$ and $m_H = 150$ GeV. Each contour represents the 1σ deviation from the SM predictions. We also show the contour of the sensitivity on $N = L\,\sigma(pp \to ggX \to HX)\mathcal{B}(H \to WW)$

as a reference.

Finally, we comment on the potential for the coupling measurements at the international linear collider. As an optional process the photon–photon collision $\gamma\gamma \to HH$ has a similar structure to $gg \to HH$ [20]. This process includes not only the top-quark loop but also the W boson loop, so that this kind of enhancement from the top–Higgs interaction may be weakened by the W boson loop. The coupling $a_{\Phi2}$ will also be measured at double-Higgs-strahlung $e^-e^+ \to ZHH$ [21], and W boson fusion $e^-e^+ \to \nu\bar{\nu}HH$ [22], as well as above the photon–photon collision [23].

Acknowledgments

APPENDIX A: CROSS SECTIONS WITH DIMENSION SIX OPERATORS

We present formulae for the single- and the double-Higgs production processes via the gluon fusion mechanism.

The hadronic cross section at the leading order is calculated by convoluting with the parton distribution function (CTEQ6M) as

$$\sigma^{\text{LO}}(gg \to H) \simeq \frac{\pi^2}{8m_H^3}\Gamma_{H\to gg}\tau \int_\tau^1 \frac{dx}{x}g(x)g(\tau/x), \tag{A1}$$

where $\tau = m_H^2/s$, and $g(x)$ is the gluon distribution function in a proton. In the SM with higher dimensional operators, the decay rate for the Higgs boson into gluons is calculated as

$$\Gamma_{H\to gg} = \frac{G_F m_H^3}{\sqrt{2}\pi}\left|a_G + \frac{\alpha_s(\mu = m_H)}{8\pi}\left(1 - \frac{a_{t1}v}{\sqrt{2}m_t}\right)\frac{4m_t^2}{m_H^2}\left[2 - m_H^2\left(1 - \frac{4m_t^2}{m_H^2}\right)C_0(m_H^2)\right]\right|^2, \tag{A2}$$

where $C_0(\hat{s}) = C_0(0, 0, \hat{s}, m_t^2, m_t^2, m_t^2)$ and $\alpha_s(\mu)$ is the running strong coupling constant. We here use the Passarino–Veltman functions for loop calculations [24]. Large higher order corrections are known for the gluon fusion mechanism [25, 26]. The next to the leading order (NLO) correction for the cross section can be treated by the K-factor [25],

$$K_{gg\to H}^{\text{NLO}} = \frac{\sigma^{\text{NLO}}(gg \to H)}{\sigma^{\text{LO}}(gg \to H)} \simeq 1 + \frac{\alpha_s(\mu)}{\pi}\left(\pi^2 + \frac{11}{2}\right). \tag{A3}$$

A naive introduction of dimension-six operator breaks renormalizability of the theory. However, these operators can be embedded in the more fundamental theory. Thus we here adopt the correction only from gluon emissions to the effective ggH vertex in the heavy top-quark mass limit as the NLO correction.

In the effective theory, loop integrations by four momenta are cut off at a some new physics scale Λ,

$$S_n^\Lambda = \frac{(4\pi)^2}{i}\int \frac{d^4k}{(2\pi)^4}\frac{1}{(k^2 - C)^n} = (-1)^n C^{2-n}\int_0^{\Lambda^2/C} dt\, \frac{t}{(1+t)^n}. \tag{A4}$$

These integrals are related to those in the dimensional regularization (DR) as

$$C_0^\Lambda = \int_0^1 dx \int_0^{1-x} dy\left[-\frac{1}{H_C}\frac{1}{(1 + H_C/\Lambda^2)^2}\right] \simeq C_0^{\text{DR}} + \frac{1}{\Lambda^2}, \tag{A5}$$

$$D_0^\Lambda = \int_0^1 dx \int_0^{1-x} dy \int_0^{1-x-y} dz\left[\frac{1}{H_D^2}\frac{1 + 3H_D/\Lambda^2}{(1 + H_D/\Lambda^2)^3}\right] \simeq D_0^{\text{DR}} - \frac{3}{2\Lambda^2}, \tag{A6}$$

16

with

$$H^C = (x\,r_1 + y\,r_2)^2 - x\,r_1^2 - y\,r_2^2 + m_t^2, \tag{A7}$$

$$H^D = (x\,r_1 + y\,r_2 + z\,r_3)^2 - x\,r_1^2 - y\,r_2^2 - z\,r_3^2 + m_t^2, \tag{A8}$$

where $r_i = \sum_i p_i$. The D_0 function will appear in the $gg \to HH$ cross section. We should comment on the reduction formulae of the loop integrals in the Passarino–Veltman technique. These reduction formulae are fully supported by Lorentz invariance, but the cut off regularization generally violates it. In our analysis, we omit the effect of the cut off Λ in the loop integrals. The corrections due to the cut off are small $(v/\Lambda)^2$ when the scale Λ is set to be more than 3 TeV, so that the effects of the error turn out to be numerically unimportant.

Let us discuss the helicity cross section for the sub-process $gg \to HH$. The differential cross section is calculated as

$$\frac{d\hat{\sigma}(g_\lambda g_{\lambda'} \to HH)}{d\hat{t}} = \frac{\left|\mathcal{M}^{\lambda\lambda'}\right|^2}{16\pi\hat{s}^2}. \tag{A9}$$

In the SM with dimension six operators $\mathcal{O}_{t1}, \mathcal{O}_{\Phi 2}$ and $\mathcal{O}_G$, helicity amplitudes $\mathcal{M}^{\lambda\lambda'}$ are given by

$$\mathcal{M}^{++} = \mathcal{M}^{--}$$
$$= \frac{\alpha_s m_t v}{\sqrt{2}\pi}\left[2 - \hat{s}\left(1 - \frac{4m_t^2}{m_H^2}\right)C_0(\hat{s})\right]\left\{\frac{3a_{t1}}{v^2} + \frac{6(\sqrt{2}m_t/v - a_{t1})}{\hat{s} - m_H^2}\left[\frac{m_H^2}{2v^2} + \frac{a_{\Phi 2}}{3}\right]\right\}$$
$$+ \frac{\alpha_s(\sqrt{2}m_t/v - a_{t1})^2}{8\pi}D_X - \frac{2a_G\hat{s}}{v^2}\left(1 + \frac{3m_H^2}{\hat{s} - m_H^2}\right) - \frac{8a_G^2\hat{s}}{v^2}, \tag{A10}$$

$$\mathcal{M}^{+-} = \mathcal{M}^{-+} = \frac{\alpha_s(\sqrt{2}m_t/v - a_{t1})^2}{8\pi}D_Y - \frac{4a_G^2(\hat{t}\hat{u} - m_H^2)}{v^2}\left(\frac{1}{\hat{t}} + \frac{1}{\hat{u}}\right), \tag{A11}$$

where $\hat{s}$, $\hat{t}$, and $\hat{u}$ are the Mandelstam variables and the box functions D_X and D_Y are defined by

$$D_X = 4\left\{2 + 4\,m_t^2\,C_0(\hat{s}) - m_t^2\left(\hat{s} + 2\,m_H^2 - 8m_t^2\right)\left(D_0^{123} + D_0^{213} + D_0^{132}\right)\right.$$
$$\left. + \frac{m_H^2 - 4\,m_t^2}{\hat{s}}\left[2\left(\hat{t} - m_H^2\right)C_0^t + 2\left(\hat{u} - m_H^2\right)C_0^u - \left(\hat{t}\hat{u} - m_H^4\right)D_0^{132}\right]\right\}, \tag{A12}$$

$$D_Y = -2\left\{-\hat{s}\,\hat{t}\,D_0^{123} - \hat{s}\,\hat{u}\,D_0^{213} + 2\,\hat{s}\,C_0(\hat{s} + 2\left(\hat{t} - m_H^2\right)C_0^t + 2\left(\hat{u} - m_H^2\right)C_0^u\right.$$
$$+ \left(\hat{s} - 2\,m_H^2 + 8m_t^2\right)\left[-2\,m_t^2\left(D_0^{123} + D_0^{213} + D_0^{132}\right) + 2\,C_0^s\right.$$
$$+ \frac{1}{\hat{t}\hat{u} - m_H^4}\left(-\hat{s}\,\hat{t}^2\,D_0^{123} - \hat{s}\,\hat{u}^2\,D_0^{213} - \hat{s}\left(\hat{s} - 2\,m_H^2\right)C_0(\hat{s})\right.$$
$$\left.\left. - \hat{s}\left(\hat{s} - 4\,m_H^2\right)C_0^s + 2\,\hat{t}\left(\hat{t} - m_H^2\right)C_0^t + 2\,\hat{u}\left(\hat{u} - m_H^2\right)C_0^u\right)\right]\right\}, \tag{A13}$$

17

where the scalar loop integrals are listed here:

$$C_0^t = C_0(0, \hat{t}, m_H^2, m_t^2, m_t^2, m_t^2), \tag{A14}$$

$$C_0^u = C_0(0, \hat{u}, m_H^2, m_t^2, m_t^2, m_t^2), \tag{A15}$$

$$C_0^s = C_0(\hat{s}, m_H^2, m_H^2, m_t^2, m_t^2, m_t^2), \tag{A16}$$

$$D_0^{123} = D_0(0, 0, m_H^2, m_H^2, \hat{s}, \hat{t}, m_t^2, m_t^2, m_t^2, m_t^2), \tag{A17}$$

$$D_0^{213} = D_0(0, 0, m_H^2, m_H^2, \hat{s}, \hat{u}, m_t^2, m_t^2, m_t^2, m_t^2), \tag{A18}$$

$$D_0^{132} = D_0(0, m_H^2, 0, m_H^2, \hat{u}, \hat{t}, m_t^2, m_t^2, m_t^2, m_t^2). \tag{A19}$$

The NLO correction for the Higgs boson pair production in the gluon fusion mechanism has been studied in the limit of the heavy top-quark mass [27]. The effect increases the cross section to 1.9–2 times that at the leading order. We here take $K_{gg \to HH}^{\mathrm{NLO}} = 1.9$ as the NLO correction to the $gg \to HH$ process.

APPENDIX B: FEYNMAN RULES

When we introduce the dimension-six genuine Higgs operators $\mathcal{O}_{\Phi 1}$ and $\mathcal{O}_{\Phi 2}$, the Feynman rules for the Higgs self-interaction are given by [14]

$$HHH : - 6\, i\, v\, Z_{\Phi 1}^3 \left(Z_{\Phi 1}^{-2} \frac{m_H^2}{2v^2} + \frac{a_{\Phi 1}}{3v^2} \sum_{j<k}^3 p_j \cdot p_k + \frac{a_{\Phi 2}}{3} \right) \tag{B1}$$

$$HHHH : - 6\, i\, Z_{\Phi 1}^4 \left(Z_{\Phi 1}^{-2} \frac{m_H^2}{2v^2} + \frac{a_{\Phi 1}}{3v^2} \sum_{j<k}^4 p_j \cdot p_k + 2 a_{\Phi 2} \right). \tag{B2}$$

In the SM with the fermionic dimension-six operator $\mathcal{O}_{t1}$, the effective top–Higgs interactions are obtained as

$$\bar{t}tH : - i\, Z_{\Phi 1} \left(\frac{m_t}{v} - \frac{a_{t1}}{\sqrt{2}} \right) \tag{B3}$$

$$\bar{t}tHH : i\, Z_{\Phi 1}^2 \frac{3 a_{t1}}{\sqrt{2} v}, \tag{B4}$$

where the wave function renormalization due to the genuine Higgs operator $\mathcal{O}_{\Phi 1}$ is also taken into account. The gluonic operator $\mathcal{O}_G$ can induce gluon–Higgs vertices at tree level as

$$G_\mu^A(p_1) G_\nu^B(p_2) H : - 2i\, Z_{\Phi 1} \frac{a_G}{v} p_1 \cdot p_2 \left(g_{\mu\nu} - \frac{p_{2\mu} p_{1\nu}}{p_1 \cdot p_2} \right) \delta^{AB} \tag{B5}$$

$$G_\mu^A(p_1) G_\nu^B(p_2) HH : - 2i\, Z_{\Phi 1}^2 \frac{a_G}{v^2} p_1 \cdot p_2 \left(g_{\mu\nu} - \frac{p_{2\mu} p_{1\nu}}{p_1 \cdot p_2} \right) \delta^{AB}. \tag{B6}$$

[1] D. Abbaneo *et al.* [LEP Collaborations and ALEPH Collaboration and DELPHI Collaboration and L3 Collaboration and LEP Electroweak Working Group and SLD Electroweak Group and SLD Heavy Flavour Group and OPAL Collaboration], arXiv:hep-ex/0412015.

[2] C. Amsler *et al.* [Particle Data Group], Phys. Lett. B **667**, 1 (2008).

[3] R. Barate *et al.* [LEP Working Group for Higgs boson searches and ALEPH Collaboration and DELPHI Collaboration and L3 Collaboration and OPAL Collaboration], Phys. Lett. B **565**, 61 (2003).

[4] R. N. Cahn and S. Dawson, Phys. Lett. B **136**, 196 (1984) [Erratum-ibid. B **138**, 464 (1984)]; D. A. Dicus and S. S. D. Willenbrock, Phys. Rev. D **32**, 1642 (1985); G. Altarelli, B. Mele and F. Pitolli, Nucl. Phys. B **287**, 205 (1987); W. Kilian, M. Kramer and P. M. Zerwas, Phys. Lett. B **373**, 135 (1996).

[5] V. Hankele, G. Klamke, D. Zeppenfeld and T. Figy, Phys. Rev. D **74**, 095001 (2006).

[6] S. L. Glashow, D. V. Nanopoulos and A. Yildiz, Phys. Rev. D **18**, 1724 (1978); J. Finjord, G. Girardi and P. Sorba, Phys. Lett. B **89**, 99 (1979); E. Eichten, I. Hinchliffe, K. D. Lane and C. Quigg, Rev. Mod. Phys. **56**, 579 (1984) [Addendum-ibid. **58**, 1065 (1986)].

[7] E. W. N. Glover and J. J. van der Bij, Nucl. Phys. B **309**, 282 (1988); D. A. Dicus, C. Kao and S. S. D. Willenbrock, Phys. Lett. B **203**, 457 (1988); T. Plehn, M. Spira and P. M. Zerwas, Nucl. Phys. B **479**, 46 (1996) [Erratum-ibid. B **531**, 655 (1998)].

[8] U. Baur, T. Plehn and D. L. Rainwater, Phys. Rev. D **69**, 053004 (2004), U. Baur, T. Plehn and D. L. Rainwater, Phys. Rev. D **67**, 033003 (2003), U. Baur, T. Plehn and D. L. Rainwater, Phys. Rev. D **68**, 033001 (2003), U. Baur, T. Plehn and D. L. Rainwater, Phys. Rev. Lett. **89**, 151801 (2002).

[9] V. A. Miransky, M. Tanabashi and K. Yamawaki, Phys. Lett. B **221**, 177 (1989); W. A. Bardeen, C. T. Hill and M. Lindner, Phys. Rev. D **41**, 1647 (1990); C. T. Hill, Phys. Lett. B **266**, 419 (1991); C. T. Hill, Phys. Lett. B **345**, 483 (1995); K. D. Lane and E. Eichten, Phys. Lett. B **352**, 382 (1995); R. S. Chivukula, E. H. Simmons and J. Terning, Phys. Lett. B **331**, 383 (1994).

[10] C. Grojean, G. Servant and J. D. Wells, Phys. Rev. D **71**, 036001 (2005); S. Kanemura, Y. Okada and E. Senaha, Phys. Lett. B **606**, 361 (2005); S. W. Ham and S. K. Oh,

arXiv:hep-ph/0502116.

[11] W. Buchmuller and D. Wyler, Nucl. Phys. B **268**, 621 (1986).

[12] K. Hagiwara, T. Hatsukano, S. Ishihara and R. Szalapski, Nucl. Phys. B **496**, 66 (1997).

[13] S. Kanemura, D. Nomura and K. Tsumura, Phys. Rev. D **74**, 076007 (2006), S. Kanemura, K. Matsuda, D. Nomura and K. Tsumura, arXiv:0710.2644 [hep-ph].

[14] V. Barger, T. Han, P. Langacker, B. McElrath and P. Zerwas, Phys. Rev. D **67**, 115001 (2003).

[15] A. Pierce, J. Thaler and L. T. Wang, JHEP **0705**, 070 (2007); E. H. Simmons, Phys. Lett. B **226**, 132 (1989).

[16] G. J. Gounaris, F. M. Renard and C. Verzegnassi, Phys. Rev. D **52**, 451 (1995).

[17] B. W. Lee, C. Quigg and H. B. Thacker, Phys. Rev. D **16**, 1519 (1977).

[18] G. J. Gounaris, D. T. Papadamou and F. M. Renard, Z. Phys. C **76**, 333 (1997).

[19] J. Pumplin, A. Belyaev, J. Huston, D. Stump and W. K. Tung, JHEP **0602**, 032 (2006).

[20] G. V. Jikia, Nucl. Phys. B **412**, 57 (1994); R. Belusevic and G. Jikia, Phys. Rev. D **70**, 073017 (2004);

[21] G. J. Gounaris, D. Schildknecht and F. M. Renard, Phys. Lett. B **83**, 191 (1979); V. D. Barger, K. m. Cheung, A. Djouadi, B. A. Kniehl and P. M. Zerwas, Phys. Rev. D **49**, 79 (1994); A. Djouadi, H. E. Haber and P. M. Zerwas, Phys. Lett. B **375**, 203 (1996); V. A. Ilyin, A. E. Pukhov, Y. Kurihara, Y. Shimizu and T. Kaneko, Phys. Rev. D **54**, 6717 (1996); J. i. Kamoshita, Y. Okada, M. Tanaka and I. Watanabe, arXiv:hep-ph/9602224; G. Belanger *et al.*, Phys. Lett. B **576**, 152 (2003).

[22] W. Kilian, M. Kramer and P. M. Zerwas, Phys. Lett. B **373**, 135 (1996); A. Djouadi, W. Kilian, M. Muhlleitner and P. M. Zerwas, Eur. Phys. J. C **10**, 45 (1999); M. Battaglia, E. Boos and W. M. Yao, in *Proc. of the APS/DPF/DPB Summer Study on the Future of Particle Physics (Snowmass 2001)* ed. N. Graf, *In the Proceedings of APS / DPF / DPB Summer Study on the Future of Particle Physics (Snowmass 2001), Snowmass, Colorado, 30 Jun - 21 Jul 2001, pp E3016*; Y. Yasui, S. Kanemura, S. Kiyoura, K. Odagiri, Y. Okada, E. Senaha and S. Yamashita, arXiv:hep-ph/0211047.

[23] F. Cornet and W. Hollik, Phys. Lett. B **669**, 58 (2008); E. Asakawa, D. Harada, S. Kanemura, Y. Okada and K. Tsumura, Phys. Lett. B **672**, 354 (2009).

[24] G. Passarino and M. J. G. Veltman, Nucl. Phys. B **160**, 151 (1979).

[25] A. Djouadi, M. Spira and P. M. Zerwas, Phys. Lett. B **264**, 440 (1991); S. Dawson, Nucl.

Phys. B **359**, 283 (1991); S. Dawson and R. Kauffman, Phys. Rev. D **49**, 2298 (1994).

[26] A. Djouadi and P. Gambino, Phys. Rev. Lett. **73**, 2528 (1994); R. V. Harlander and W. B. Kilgore, Phys. Rev. Lett. **88**, 201801 (2002), JHEP **0210**, 017 (2002); C. Anastasiou and K. Melnikov, Nucl. Phys. B **646**, 220 (2002); V. Ravindran, J. Smith and W. L. van Neerven, Nucl. Phys. B **665**, 325 (2003); S. Catani, D. de Florian, M. Grazzini and P. Nason, JHEP **0307**, 028 (2003); U. Aglietti, R. Bonciani, G. Degrassi and A. Vicini, Phys. Lett. B **595**, 432 (2004); G. Degrassi and F. Maltoni, Phys. Lett. B **600**, 255 (2004); S. Moch and A. Vogt, Phys. Lett. B **631**, 48 (2005); V. Ravindran, Nucl. Phys. B **746**, 58 (2006), Nucl. Phys. B **752**, 173 (2006); S. Actis, G. Passarino, C. Sturm and S. Uccirati, Phys. Lett. B **670**, 12 (2008); S. Marzani, R. D. Ball, V. Del Duca, S. Forte and A. Vicini, Nucl. Phys. B **800**, 127 (2008), Nucl. Phys. Proc. Suppl. **186**, 98 (2009).

[27] S. Dawson, S. Dittmaier and M. Spira, Phys. Rev. D **58**, 115012 (1998).